Cell Metabolism, Volume *26*

Supplemental Information

Cold-Induced Thermogenesis Depends on ATGL-Mediated Lipolysis in Cardiac Muscle, but Not Brown Adipose Tissue

Renate Schreiber, Clemens Diwoky, Gabriele Schoiswohl, Ursula Feiler, Nuttaporn Wongsiriroj, Mahmoud Abdellatif, Dagmar Kolb, Joris Hoeks, Erin E. Kershaw, Simon Sedej, Patrick Schrauwen, Guenter Haemmerle, and Rudolf Zechner

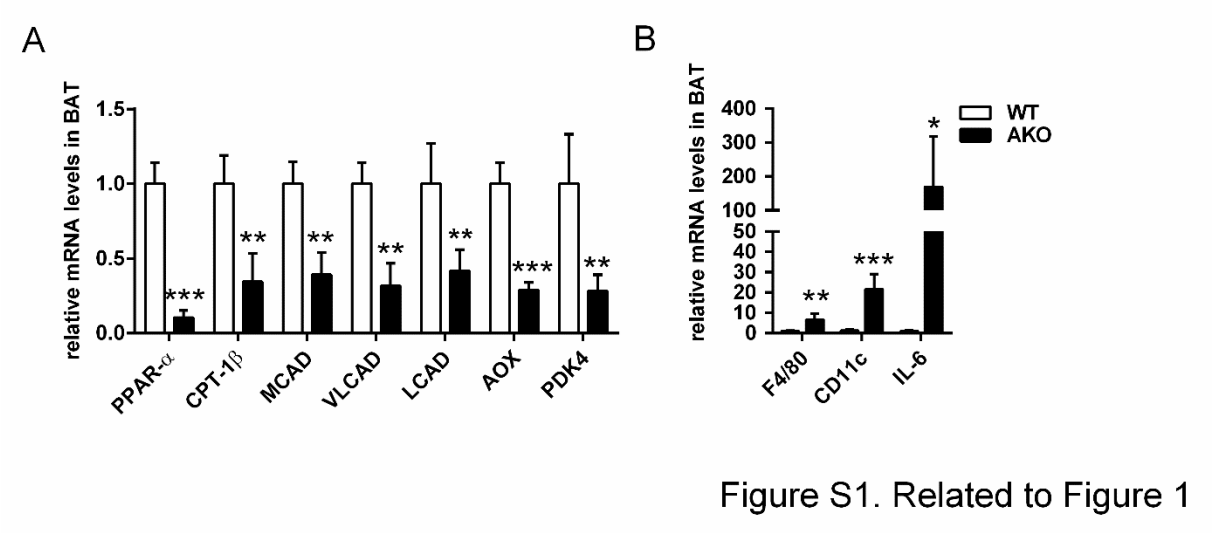

Figure S1. Related to Figure 1

Figure S1. Global ATGL deficiency causes cold-induced hypothermia and BAT hypertrophy, but does not alter mitochondrial function in BAT. Related to Figure 1.

(A) Relative mRNA expression of PPAR-α and its target genes in BAT (*n* = 5).

(B) Relative mRNA expression of inflammation markers in BAT (*n* = 5).

Gene expression analyses were performed in BAT from male mice aged 9–10 weeks upon cold exposure at 5°C for 3–6 hr. Data are presented as means ± SD. Statistical significance was evaluated by unpaired, two-tailed Student's t test. *, $p < 0.05$, **, $p < 0.01$, and ***, $p < 0.001$.

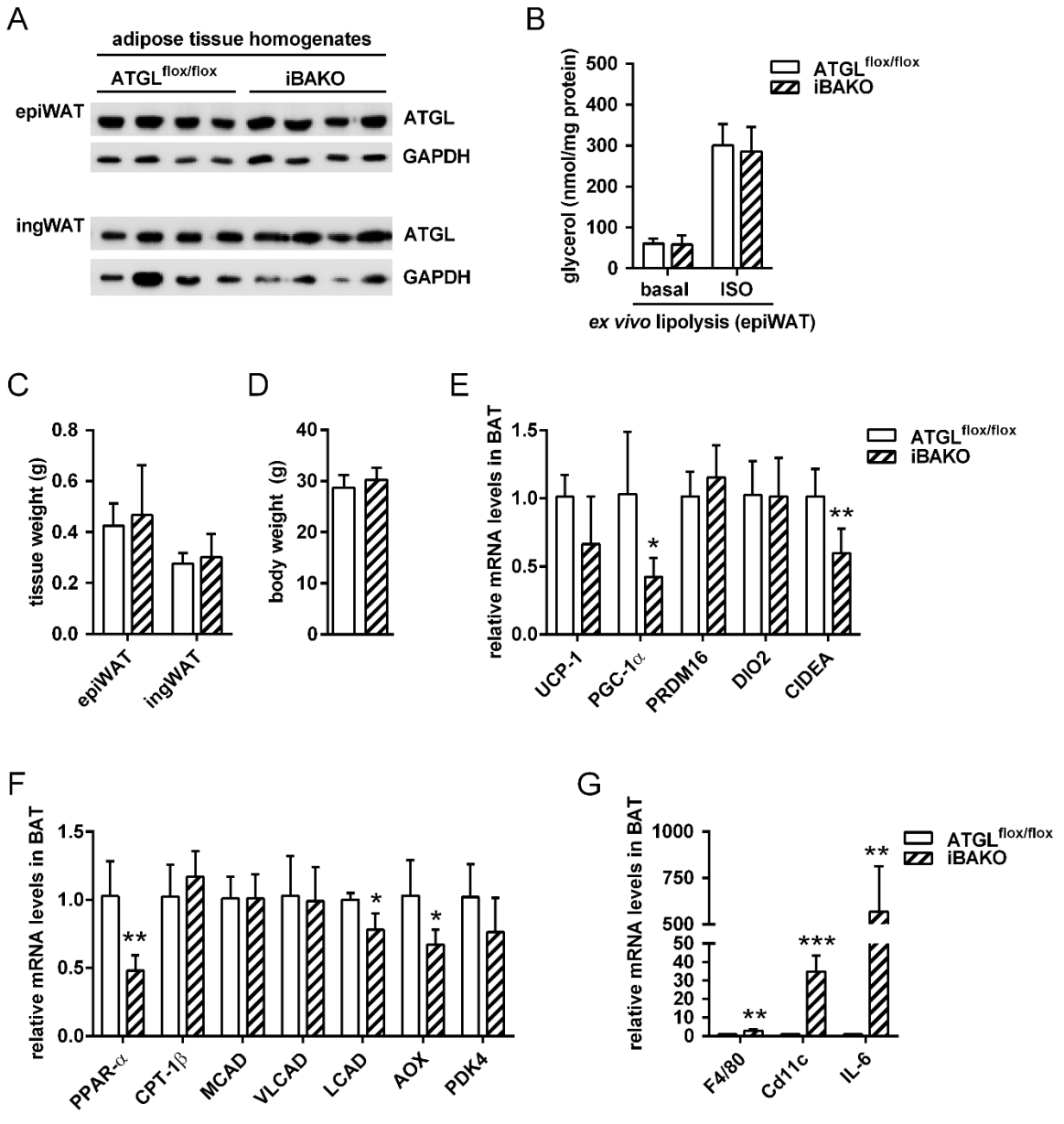

Figure S2. Related to Figure 2

Figure S2. ATGL in BAT is not essential for thermogenesis during acute cold. Related to Figure 2.

(A) ATGL immunoblot of epiWAT and ingWAT homogenates.

(B) *Ex vivo* lipolysis from epiWAT under basal and isoproterenol (ISO)-stimulated conditions (n = 4).

(C) Tissue weights (n = 6).

(D) Body weight (n = 11).

(E) Relative mRNA expression of BAT-specific genes in BAT (n = 5).

(F) Relative mRNA expression of PPAR-α and its target genes in BAT (n = 5).

(G) Relative mRNA expression of inflammation markers in BAT (n = 5).

Analyses were performed in male mice aged 9–11 weeks and 4-weeks upon tamoxifen administration. Protein expression and *ex vivo* lipolysis were performed in tissues derived from mice housed at normal housing temperatures at 22°C–23°C. Gene expression analyses were performed in BAT from mice exposed to cold at 5°C for 6 hr. Data are presented as means ± SD. Statistical significance was evaluated by unpaired, two-tailed Student's t test or two-way ANOVA with Bonferroni post-hoc tests. *, $p < 0.05$, **, $p < 0.01$, and ***, $p < 0.001$.

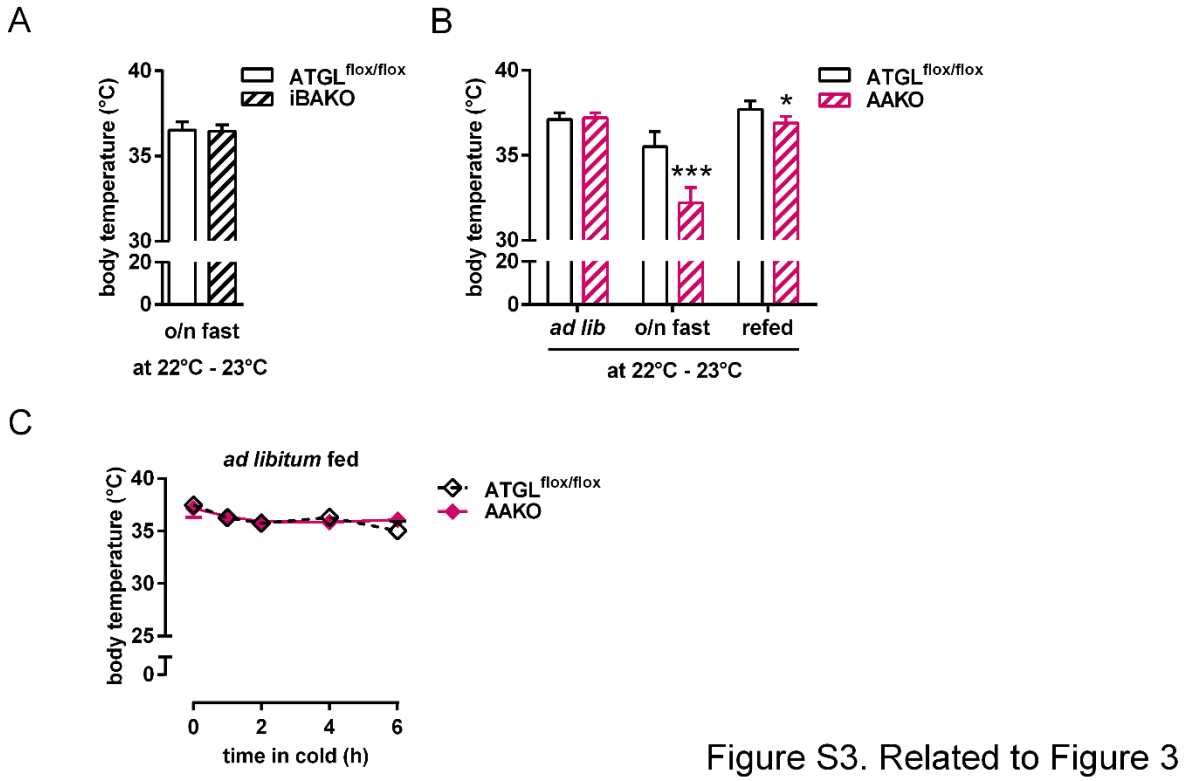

Figure S3. Related to Figure 3

Figure S3. ATGL-mediated lipolysis in WAT is essential to fuel thermogenesis during fasting. Related to Figure 3.

(A) Body temperature of mice of mixed sex aged 10–12 weeks and 4-weeks upon tamoxifen administration after an overnight (o/n) fast for 12 hr at 22°C–23°C (*n* = 5–6).

(B) Body temperature of male mice aged 10–12 weeks in the *ad libitum* fed (*ad lib*), o/n fasted for 12 hr, and refeeding state for 1 hr at 22°C–23°C (*n* = 6–7).

(C) Body temperature of male mice aged 16 weeks in the *ad libitum* fed state during acute cold exposure at 5°C (*n* = 5).

Data are presented as means ± SD. Statistical significance was evaluated by unpaired, two-tailed Student's t test. *, $p < 0.05$ and ***, $p < 0.001$.

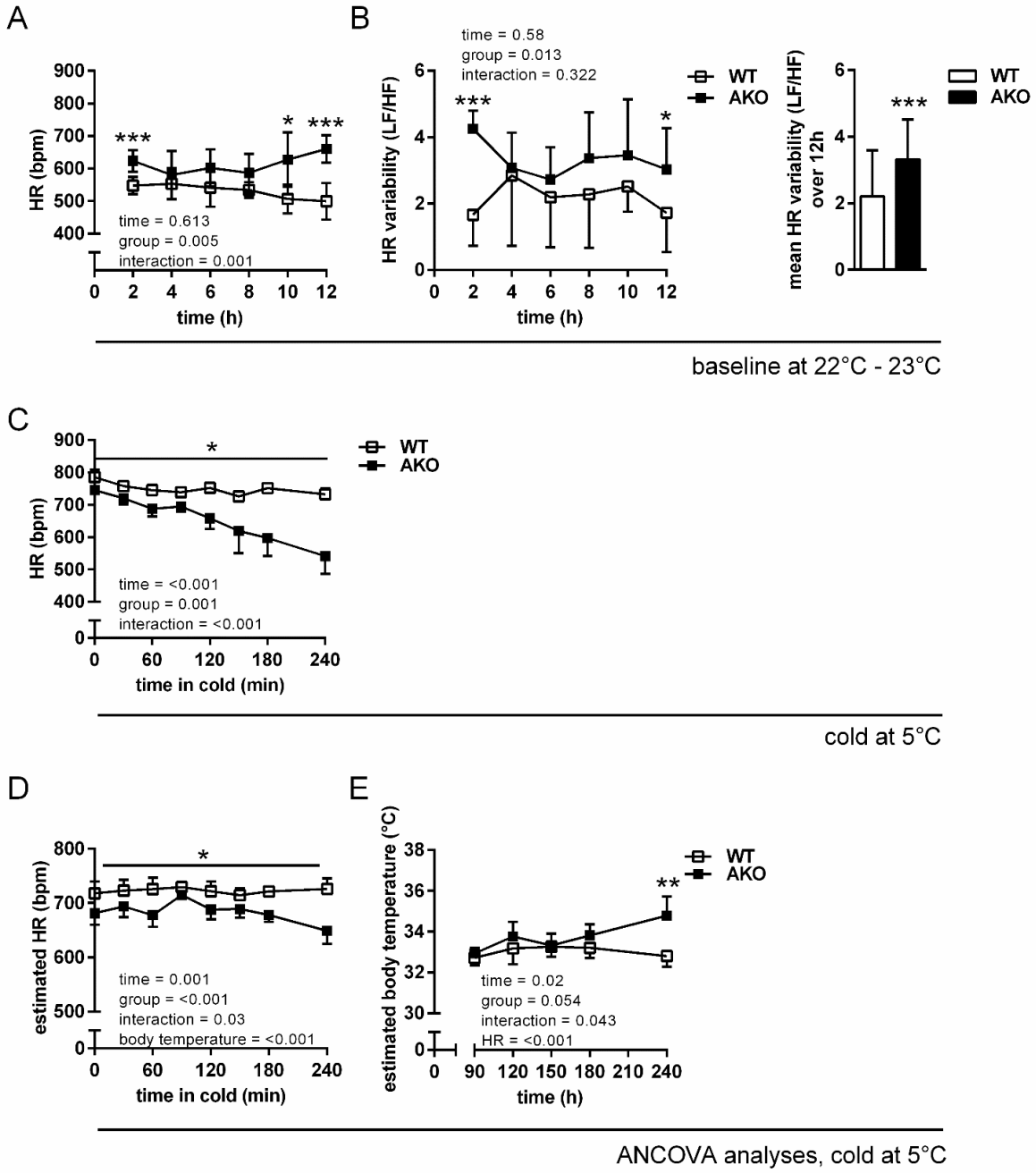

Figure S4. Related to Figure 4

Figure S4. Impaired heart function due to cardiac ATGL deficiency causes hypothermia. Related to Figure 4.

(A) Heart rate (HR) under baseline at normal housing temperatures at 22°C–23°C (*n* = 6).

(B) HR variability (ratio of low-to-high frequency, LF/HF) during normal housing temperatures at 22°C–23°C. Time-course (left) and mean over the whole analyses period of 12 hr (right, *n* = 6).

(C) HR upon acute cold exposure at 5°C (*n* = 4).

(D) Estimated HR at a hypothetical body temperature of 34°C (*n* = 4).

(E) Estimated body temperature for corrected HR of 689 bpm (*n* = 4).

HR analyses were performed using telemetry transmitters in male mice aged 8 weeks. Data are presented as means ± SD. Statistical significance was evaluated by two-way ANOVA (A – C) or unpaired, two-tailed Student's t test (B, right graph). ANCOVA was used to analyze estimated HR and body temperature (D – E). *, $p < 0.05$, **, $p < 0.01$ and ***, $p < 0.001$.

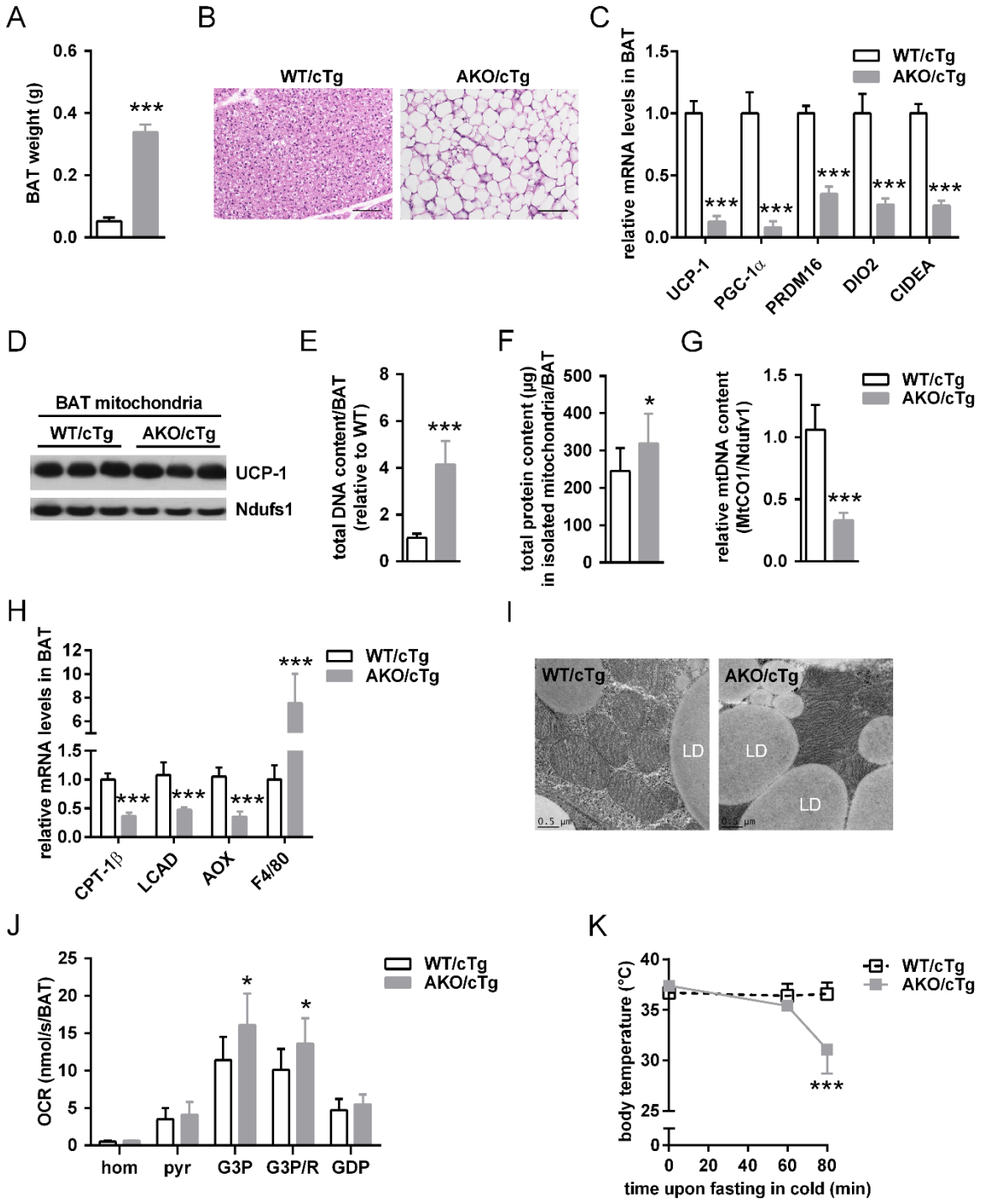

Figure S5 - Related to Figure 4

Figure S5. Impaired heart function due to cardiac ATGL deficiency causes hypothermia. Related to Figure 4.

(A) BAT weight (n ≥ 5).

(B) Histology of BAT. Scale bar, 100 µm.

(C) Relative mRNA expression of classical brown fat genes upon acute cold exposure (*n* = 6).

(D) UCP-1 immunoblot of isolated BAT mitochondria upon acute cold exposure.

(E) Total DNA content in whole BAT depots (*n* = 6).

(F) Total protein content in isolated mitochondria from whole BAT depots (*n* = 10).

(G) Relative mitochondrial (mt) DNA content in BAT assessed by qPCR and calculated from copy number of the mtDNA encoded MtCO1 gene and the nuclear DNA encoded Ndufv1 gene (*n* = 6).

(H) Relative mRNA expression of PPAR-α targets and inflammation marker upon acute cold exposure (*n* = 6).

(I) Representative transmission electron micrographs from BAT. Scale bar, 0.5 µm.

(J) Oxygen consumption rates (OCR) in BAT homogenates (hom) using pyruvate (pyr), glycerol-3-P in the absence (G3P) and presence of rotenone (G3P/R), and guanosine 5'-diphosphate (GDP). OCR were calculated for whole BAT depots (*n* = 8–9).

(K) Body temperature during fasting at 5°C for indicated time points (*n* = 5–6).

Male mice aged 8–12 weeks were used, except for (J) using mice of mixed sex and (K) using female mice aged 12–16 weeks. Data are presented as means ± SD. Statistical significance was evaluated by unpaired, two-tailed Student's t test. *, $p < 0.05$, **, $p < 0.01$ and ***, $p < 0.001$.

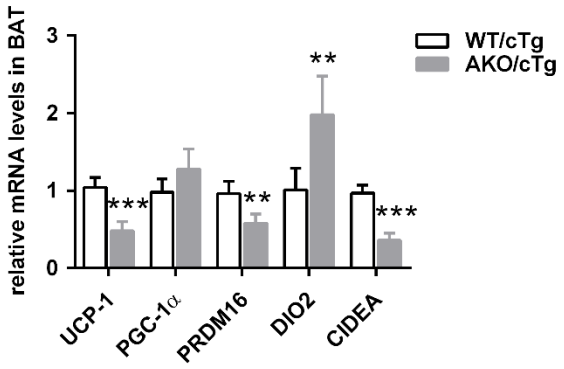

Figure S6. Related to Figure 5

Figure S6. ATGL-deficient mice survive upon cold acclimation and exhibit normal brown adipocyte recruitment. Related to Figure 5.

Relative mRNA expression in BAT from AKO/cTg mice upon cold acclimation at 5°C for 3 weeks (*n* = 5).

Analyses were performed from *ad libitum* fed male AKO/cTg mice aged 10–12 weeks. Data are presented as means ± SD. Statistical significance was evaluated by unpaired, two-tailed Student's t test. *, $p < 0.05$, **, $p < 0.01$, and ***, $p < 0.001$.

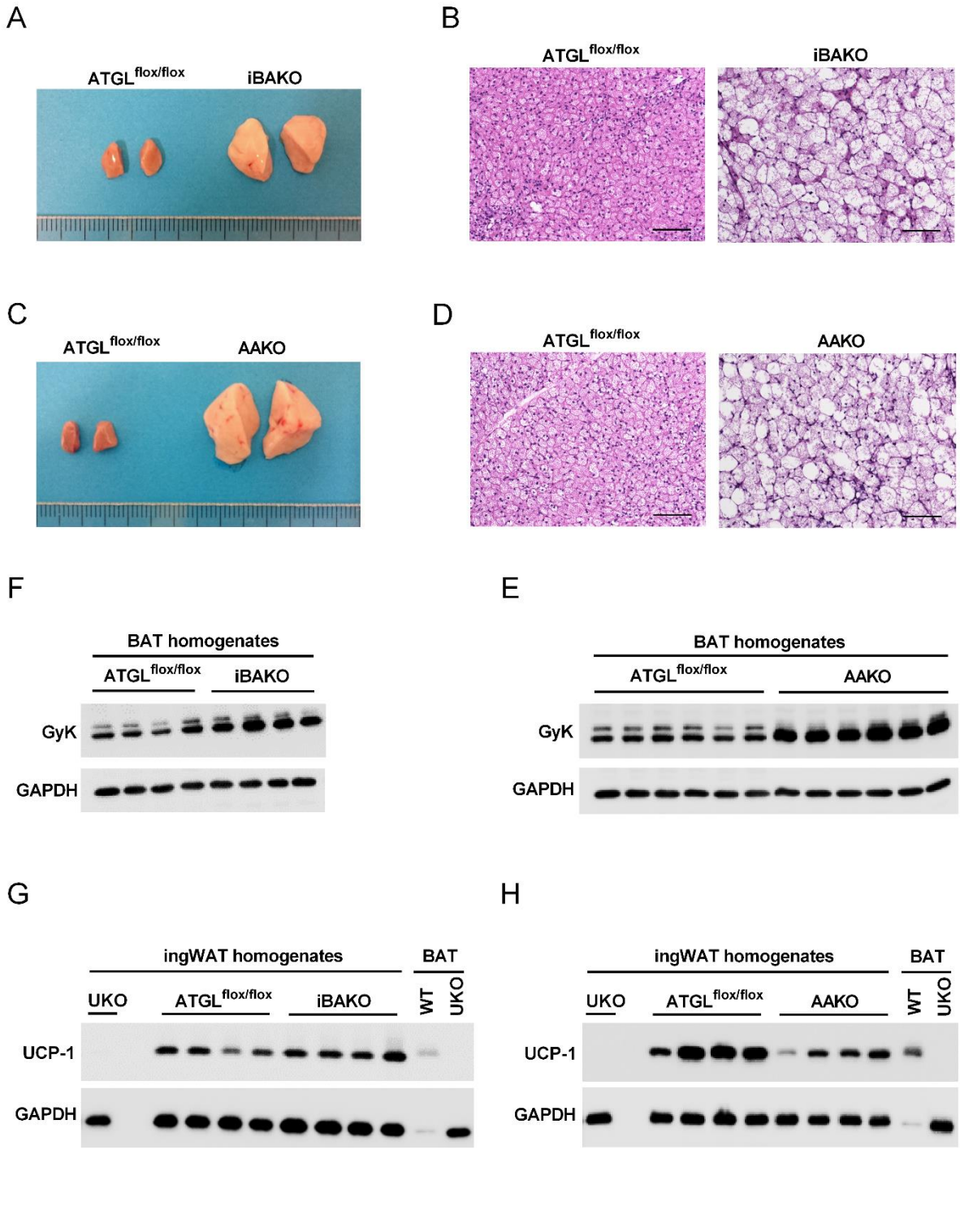

Figure S7. Related to Figure 6

Figure S7. Adaptive NST is intact in ATGL-deficient BAT. Related to Figure 6.

(A, C) Gross morphology of BAT from iBAKO (A) and AAKO mice (C).

(B, D) Representative histology image of BAT from iBAKO (B) and AAKO mice (D). Scale bar, 100 µm.

(F, E) Glycerol Kinase (GyK) immunoblot from BAT homogenates derived from iBAKO (F) and AAKO mice (E).

(G, H) UCP-1 immunoblot of ingWAT homogenates from iBAKO (G) and AAKO mice (H). For all ingWAT samples, 20 µg protein were loaded per lane. BAT derived from cold-acclimatized WT (5 µg protein per lane) and UCP-1 knockout mice (UKO; 20 µg protein per lane) were used as positive and negative controls, respectively.

All mice were acclimatized to cold at 5°C for 3 weeks. Tissues and tissue homogenates were derived from male mice aged 12–16 weeks and 4-weeks upon tamoxifen administration (iBAKO).

Table S1. Plasma parameters of mutant mice upon acute cold exposure. Related to Figure 4. Data are shown from male iHAKO at indicated periods of time upon tamoxifen administration (postTAM) (*n* = 5–9). Plasma parameters were determined from *ad libitum* fed mice upon acute cold exposure at 5°C. Data are presented as means ± SD. Statistical significance was evaluated by unpaired, two-tailed Student's t test. *, $p < 0.05$ and **, $p < 0.01$.

postTAM	plasma levels	genotype	
6-weeks		**ATGL$^{flox/flox}$**	**iHAKO**
	glucose (mg/dl)	205 ± 15	219 ± 27
	FA (mM)	0.35 ± 0.08	0.30 ± 0.10
	TG (mM)	0.29 ± 0.06	0.30 ± 0.12
10-weeks			
	glucose (mg/dl)	204 ± 19	248 ± 30*
	FA (mM)	0.39 ± 0.11	1.02 ± 0.20**
	TG (mM)	0.26 ± 0.15	0.68 ± 0.13**

Table S2. Body weight, body composition, plasma parameters, and food intake of mutant mice upon cold acclimation. Related to Figure 6. Data are shown from male AKO/cTg mice aged of 10–12 weeks (*n* = 5–6), male iBAKO mice aged 12–15 weeks and 5-weeks upon tamoxifen administration (*n* = 5–11), and male AAKO mice aged 12 weeks (*n* = 6). All mice were acclimatized to cold at 5°C for 3 weeks. Plasma parameters were determined from mice fed *ad libitum*. Data are presented as means ± SD. Statistical significance was evaluated by unpaired, two-tailed Student's t test. *, $p < 0.05$, ***, $p < 0.001$.

analyzed parameter	genotypes	
body composition	**WT/cTg**	**AKO/cTg**
body weight, g	23.1 ± 0.8	24.6 ± 1.5
iBAT mass, mg	112 ± 13	622 ± 32***
epiWAT mass, mg	208 ± 22	416 ± 55***
ingWAT mass, mg	180 ± 18	614 ± 65***
heart, mg	148 ± 12	150 ± 19
quadriceps, mg	327 ± 36	302 ± 34
energy substrate levels and food intake		
plasma glucose (mg/dl)	192 ± 210	194 ± 27
plasma FA (mM)	0.60 ± 0.12	0.28 ± 0,04*
plasma TG (mM)	0.50 ± 0.05	0.50 ± 0.08
food intake (g), light	1.1 ± 0.3	2.0 ± 0.5*
food intake (g), dark	6.1 ± 0.2	5.6 ± 0.2*
body composition	**$ATGL^{flox/flox}$**	**iBAKO**
body weight, g	28.9 ± 1.3	29.0 ± 1.4
iBAT mass, mg	109 ± 11	479 ± 26***
epiWAT mass, mg	285 ± 67	171 ± 25*
ingWAT mass, mg	240 ± 34	301 ± 56
heart, mg	165 ± 2	172 ± 15
quadriceps, mg	339 ± 66	321 ± 19
energy substrate levels and food intake		
plasma glucose (mg/dl)	193 ± 26	174 ± 21
plasma FA (mM)	0.39 ± 0.12	0.45 ± 0.19
plasma TG (mM)	0.51 ± 0.21	0.66 ± 0.27
food intake (g), light	1.3 ± 0.4	1.4 ± 0.4
food intake (g), dark	6.8 ± 0.9	7.6 ± 1.2
body composition	**$ATGL^{flox/flox}$**	**AAKO**
body weight, g	27.2 ± 1.1	29.3 ± 1.4*
iBAT mass, mg	99 ± 11	840 ± 132***
epiWAT mass, mg	214 ± 30	440 ± 120**
ingWAT mass, mg	193 ± 34	655 ± 93***
heart, mg	164 ± 19	163 ± 15
quadriceps, mg	339 ± 14	282 ± 34**
energy substrate levels and food intake		
plasma glucose (mg/dl)	204 ± 25	172 ± 19*
plasma FA (mM)	0.35 ± 0.12	0.26 ± 0,05*
plasma TG (mM)	0.48 ± 0.26	0.38 ± 0.17
food intake (g), light	1.3 ± 0.3	2.3 ± 0.2***
food intake (g), dark	6.0 ± 0.3	5.4 ± 0.3*

Table S3. Primers used for relative gene expression and mtDNA content. Related to STAR methods.

Synonym	Gene	Primer sequences, fwd/rev
UCP-1	Uncoupling protein-1	5'-ACTGCCACACCTCCAGTCATT-3' 5'-CTTTGCCTCACTCAGGATTGG-3'
PGC-1α	PPAR-g co-activator 1a	5'-CAGCACGGTGAAGCCATTC-3' 5'-TGCTGCTGTTCCTGTTTTC-3'
PRDM16	PR domain containing 16	5'-CAGCACGGTGAAGCCATTC-3' 5'-GCGTGCATCCGCTTGTG-3'
DIO2	Type II deiodinase	5'-CAGTGTGGTGCACGTCTCCAATC-3' 5'-TGAACCAAAGTTGACCACCAG-3'
CIDEA	Cell death-inducing DFFA-like effector A	5'-TGCTCTTCTGTATCGCCCAGT-3' 5'-GCCGTGTTAAGGAATCTGCTG-3'
PPAR-α	Peroxisome proliferator activated receptor alpha	5'-GTACCACTACGGAGTTCACGCAT-3' 5'-CGCCGAAAGAAGCCCTTAC-3'
CPT-1β	Carnitine palmitoyl-transferase 1B	5'-CGAGGATTCTCTGGAACTGC-3' 5'-GGTCGCTTCTTCAAGGTCTG-3'
MCAD	Medium chain acyl-CoA dehydrogenase	5'-CAACACTCGAAAGCGGCTCA-3' 5'-ACTTGCGGGCAGTTGCTTG-3'
LCAD	Long chain acyl-CoA dehydrogenase	5'-GGCAAAATACTGGGCATCTGA-3' 5'-CTCCGTGGAGTTGCACACAT-3'
VLCAD	Very long chain acyl-CoA dehydrogenase	5'-ACCTTGCCAGGGCCTGAT-3' 5'-TGGCCTGGTCACCGGTAA-3'
AOX	Acyl CoA oxidase 1	5'-AGATTGGTAGAAATTGCTGCAAAA-3' 5'-ACGCCACTTCCTTGCTCTTC-3'
PDK4	Pyruvate dehydrogenase kinase 4	5'-ATCTAACATCGCCAGAATTAAACC-3' 5'-GGAACGTACACAATGTGGATTG-3'
F4/80	F4/80	5'-GGATGTACAGATGGGGGATG 5'-CATAAGCTGGGCAAGTGGTA
CD11c	Integrin, alpha X	5'-CAGTGACCCCGATCACTCTT 5'-CACCACCAGGGTCTTCAAGT
IL-6	Interleukin 6	5'-GAGGATACCACTCCCAACAGACC-3' 5'-CAGCTCCAACAGCCTTACTACGT -3
TBP	TATA binding protein	5'-GAAGCTGCGGTACAATTCCAG-3' 5'-CCCCTTGTACCCTTCACCAAT-3'
36B4	Ribosomal protein, large, P0 (Rplp0)	5'-AGCCATGTACGTAGCCATCCA -3' 5'-TCTCCGGAGTCCATCACAATG -3'
MtCO1	Mitochondrial DNA encoded cytochrome c oxidase 1	5'-TGCTAGCCGCAGGCATTAC-3' 5'-GGGTGCCCAAAGAATCAGAAC-3'
Ndufv1	Nuclear DNA encoded NADH dehydrogenase	5'-CTTCCCCACTGGCCTCAAG-3' 5'-CCAAAACCCAGTGATCCAGC-3'